Published in final edited form as:
Biochemistry. 2011 April 19; 50(15): 3045–3047. doi:10.1021/bi200336b.

Homo sapiens Dullard Protein Phosphatase Shows Preference Toward Insulin-dependent Phosphorylation Site of Lipin1†

Rui Wu[‡], **Megan Garland**[‡], **Debra Dunaway-Mariano**[§,*], and **Karen N. Allen**[‡,*]

[‡]Department of Chemistry, Boston University, 590 Commonwealth Avenue, Boston, MA 02215

[§]Department of Chemistry and Chemical Biology, University of New Mexico, Albuquerque, NM 87131

Abstract

Human lipin1 catalyzes the highly regulated conversion of phosphatidic acids to diacylglycerides. Lipin's cellular location, protein partners, and biological function are directed by phosphorylation/dephosphorylation events catalyzed by the phosphoserine phosphatase dullard. To define the determinants of dullard substrate recognition and catalysis, and hence, lipin regulation, steady-state kinetic analysis was performed on phosphoserine-bearing nonapeptides based on the phosphorylation sites of lipin. The results demonstrate that dullard shows specificity toward the peptide corresponding to the insulin-dependent phosphorylation site (Ser106) of lipin with $k_{cat}/K_m = 1 \times 10^4\ M^{-1}\ s^{-1}$. These results are consistent with a coil/loop structure for the insulin-dependent phosphorylation site on human lipin1 and make the requirement for an adaptor protein to confer activity such as that proposed for the yeast homologue, unlikely.

Keywords

protein phosphoserine phosphatase; HAD superfamily; phosphatidic acid phosphatase

Human lipin acts as a phosphatidic acid (PA) phosphohydrolase(1). It is considered to be one of the key regulators of cellular lipid metabolism in myelinated motor neurons and in a variety of tissues including adipose, liver, and muscle (2–4). Three lipin isoforms exist in higher eukaryotes, dubbed lipin1, lipin2 and lipin3. Identification of the genetic mutation responsible for the fatty liver dystrophic mouse phenotype(1) led to a single-site mutation in the lipin1 protein (Gly84Arg) and ultimately to the assignment of its catalytic activity. Polymorphisms in the lipin1 and lipin 2 genes are associated with various disease states(5–8). Notably, a variation in the lipin1 gene that causes an amino-acid substitution within the phosphatase catalytic domain is linked to statin-induced myopathy(9). Lipin1 is a large (890 residues in human), multidomain protein comprised of a predicted N-terminal domain (NLIP) of unknown structure, an intervening segment that includes a serine-rich domain, and a C-terminal phosphatase domain which are homologous (Figure 1) to the catalytic

[†]Abbreviations: CTD, C-terminal domain; ER, endoplasmic reticulum; HADSF, haloalkanoate dehalogenase superfamily, MESG, 2-amino-6-mercapto-7-methylpurine riboside; NLIP, lipin N-terminal domain; PA, phosphatidic acid; pSer, Oγ-phosphory serine; pS, Oγ-phosphory serine ; pNPP, p-nitrophenyl phosphate.

[*]To whom correspondence should be addressed. K.N.A.: drkallen@bu.edu. Phone 617-358-5544. Fax: 202-354-5386; D.D-M.: dd39@unm.edu. Fax (505) 277-2609.

SUPPORTING INFORMATION AVAILABLE

Figures S1–S3 showing sequence alignments and protein purity as well as detailed protocols for cloning, expression, purification, and steady-state kinetics are provided. This material is available free of charge via the Internet at http://pubs.acs.org.

domain of the haloalkanoate dehalogenase superfamily (HADSF), a large ubiquitous superfamily made up mostly of phosphatases(10–11).

Phosphorylation is a regulator of lipin1 cellular location. In humans, a specific phosphatase, dullard, catalyzes the hydrolysis of lipin Oγ-phosphoryl serines (pSer). Similarly, the yeast orthologue of dullard, Nem1, acts on the yeast lipin orthologue Smp2(12). Notably, dullard/Nem1 are also members of the HADSF. Sequence analysis shows that although they differ in length (244 and 446 residues for human dullard and *Saccharomyces cerevisiae* Nem1, respectively) each is comprised of a N-terminal 22-amino acid transmembrane helix and a C-terminal HADSF domain that conserves all four of the expected catalytic motifs involved in phosphoryl transfer. Alignment of human dullard and *S. cerevisiae* Nem1 HADSF domains (residues 235–446) shows that they are homologous with 44% sequence identity with 68% sequence similarity. The phosphatase activity of dullard/Nem1 is intimately linked to the function of lipin1/Smp2(13–14). Yeast cells lacking active Nem1 phosphatase exhibit the phenotype characteristic of Smp2 knock-out, namely, derepression of phospholipid synthesis genes and massive expansion of the nuclear membrane and endoplasmic reticulum (ER) membrane(12). Lipin phosphorylation is hypothesized to prevent substrate accessibility to the ER and nuclear membranes, yet to have no impact on the PA hydrolase activity. A survey measuring relative activities of dullard toward an array of 360 phosphopeptides *in vitro* showed a marked preference for dullard toward pSer-containing peptides over phosphothreonine- or phosphotyrosine-containing peptides(14). Although numerous sites of phosphorylation have been identified in lipin1 and yeast Smp2, Ser106 of lipin1 appears to be a major site of insulin-stimulated phosphorylation(15). The preference of dullard/Nem1 for one pSer site over another has not been examined.

An apparent paradox discovered upon analyzing the *in vitro* activities of Nem1 and dullard is the dependence of Nem1 activity in yeast on the presence of the protein Spo7, a multi-pass integral membrane protein. Reportedly, based on pull-down experiments Spo7 was found to bind to Nem1 at the C-terminal catalytic domain. Furthermore, deletion of Spo7 leads to a similar phenotype as deletion of Nem1, resulting in the accumulation of the phosphorylated form of Smp2 and nuclear membrane proliferation(16). Moreover, in the presence but not the absence of Spo7, Nem1 shows *in vitro* catalytic activity against p-nitrophenyl phosphate (pNPP)(12). Based on the current understanding of HADSF phosphatase structure and mechanism, it is unclear how Spo7 might stimulate Nem1 catalyzed dephosphorylation of pNPP.

Herein, we provide steady-state kinetic evidence that heterologously expressed human dullard (lacking the N-terminal transmembrane helix) acts on nonapeptides corresponding to the human lipin1 sequence with high specificity toward the peptide corresponding to the sequence flanking Ser106. The *in vitro* activity of the human dullard shows no requirement for a Spo7 orthologue.

We began our study of the dullard-lipin1 interaction by creating and examining a model of the three-dimensional structure of dullard. The objective was to determine whether the dullard active site is configured to bind an extended versus folded pSer-bearing sequence. Accordingly, a sequence homology threading model was generated in PHYRE using as the template the structure of the RNA polymerase C-terminal domain (CTD) phosphatase, Scp1 (PDB 1TA0; spanning residues 77–256 that comprise the HADSF domain)(17) which bears 45 % sequence identity to dullard. Residues 46–244 corresponding to the dullard sequence minus the N-terminal transmembrane helix were modeled. The high sequence identity and lack of extensive gaps in the alignment of the two sequences (Figure S1) is indicative of a reliable model. In addition to the sequence similarity, there is similarity in the physiological functions of Scp1 and dullard, as Scp1 dephosphorylates the pSer5 site on the C-terminal

domain of RNA polymerase(18). HADSF members dullard and Scp1 are expected to share the same catalytic domain architecture, which includes the active site DXD nucleophile/general acid/base and the Mg^{2+} binding motifs essential for phosphoryl transfer(10). The model for dullard has similar accessibility to the active site compared to other proteins in the HADSF that are believed to form a protein-protein(19) or protein-polynucleotide(20) interface (Figure 2). This finding is consistent with either a protein surface interaction between dullard and lipin or an extended peptide chain interaction.

If dullard is similar to Scp1 in its mode of substrate recognition, it is expected that there will be conservation of the substrate-binding residues in the active-site. The mode of substrate binding and the specificity determinants of Scp1 have been revealed via X-ray crystal structures of an inactive Scp1-D96N mutant (oblating phosphoaspartyl intermediate formation) bound with pSer containing 9- and 14-mer peptides, which incorporate selected regions of the RNA polymerase CTD sequence (21). The structures are consistent with a mode of interaction in which the extended RNA polymerase CTD threads through the Scp1 active-site canyon. Peptide binding is conferred by coordination of the phosphoryl group by the cofactor Mg^{2+} and by interactions with a hydrophobic groove formed between the catalytic domain and the inserted segments (comprised of Phe106, Val118, Ile120, Val127, and Leu155)(21). Mapping of the stringently conserved residues of dullard obtained from a sequence alignment of all eukaryotic orthologues (Figure S2) onto the homology model of dullard shows that the substrate-binding cleft is retained (Figure 3), with a similar active site groove comprised of residues His77, Val97, Ile99, Phe106, and Met134 stringently conserved among vertebrates. The mode and site of pSer peptide binding is then, most likely conserved between Scp1 and dullard. Because this finding indicates that dullard is targeting pSer residues located on solvated regions that are free to associate with the peptide-binding cleft, a kinetic analysis of nonapeptides based on lipin pSer sites was undertaken.

Dullard, lacking the N-terminal transmembrane domain (dullard 46–244, consistent with that portion of dullard modeled) was prepared as a recombinant protein and heterologously expressed in *E. coli* (see Supporting Information). The resulting >95% pure (as assessed by SDS/PAGE) dullard 46–244 was used in steady-state kinetic experiments to determine the specificity constants (k_{cat}/K_m) for dullard-catalyzed dephosphorylation of lipin derived pSer peptides. Based on the documented specificity of Scp1 for SPTpSP peptides(21) and the conservation of a substantial fraction of the residues that form the peptide binding pocket in dullard and Scp1, Pro/Thr/Ser containing phosphoserine nonapeptides that represent lipin phosphorylation sites(22–24) were tested as substrates. The 2-amino-6-mercapto-7-methylpurine riboside (MESG)-coupled phosphatase assay (Enzcheck assay kit) and molybdate green assay (Biomol Green assay kit) were employed as independent methods for monitoring dullard-catalyzed phosphate release from peptides.

The steady-state kinetic results (Table 1) are consistent with recognition by dullard of specific solvated regions of lipin1 and with dullard specificity similar to that of the CTD phosphatase. The highest k_{cat}/K_m value (2.9×10^4 M^{-1} s^{-1}) was obtained for the peptide corresponding to the insulin dependent phosphorylation site at Ser 106, HLAT(pS)PILS. The reactivity of dullard toward the S106 peptide was ~40 times greater in k_{cat}/K_m than the next most reactive peptide (S248). In comparison, dullard-catalyzed hydrolysis of the "generic" substrate pNPP has a low k_{cat}/K_m of 56 M^{-1} s^{-1} (k_{cat} = 1 s^{-1} and K_m = 18 mM) (14). The specificity of dullard is similar to that of Scp1 for its preferred peptide substrates (e.g. $k_{cat}/K_m = 1.0 \times 10^4$ M^{-1} s^{-1} for YSPT(pS)PS)(21). Notably, the preference for the sequence T(pS)P is shared between the two phosphatases. Taken together, these results suggest that dullard is targeting pSer106 and that this insulin-dependent phosphorylation site is most likely located within an unstructured (i.e., extended and solvated) region of lipin.

Indeed, Ser106 is located in a region at the C-terminal end of the NLIP domain(1) with no predicted structure (Figure 1).

The specificity and high catalytic efficiency of dullard toward lipin-derived peptides measured by the *in vitro* assays herein suggest that human dullard does not require an adaptor/accessory protein for activity. Notably, whereas Spo7 homologs are pervasive in yeast and plant species, we were unable to identify such a Spo7 homolog in human. The observation that dullard/Nem1 as well as Spo7 are predicted to be membrane-bound, and the phosphorylated substrate lipin/Smp2 are cytosolic proteins, introduces an intriguing possibility- that of regulation of activity by proximity. In yeast Spo7 is posited to function as an essential adapter. In human such an adapter if it exists, remains to be discovered.

Supplementary Material

Refer to Web version on PubMed Central for supplementary material.

Acknowledgments

This work was supported by National Institutes of Health Grant GM061099 and GM093342 (to K.N.A and D.D-.M.).

REFERENCES

1. Peterfy M, Phan J, Xu P, Reue K. Nat Genet. 2001; 27:121. [PubMed: 11138012]
2. Finck BN, Gropler MC, Chen Z, Leone TC, Croce MA, Harris TE, Lawrence JC Jr, Kelly DP. Cell Metab. 2006; 4:199. [PubMed: 16950137]
3. Peterfy M, Phan J, Reue K. J Biol Chem. 2005; 280:32883. [PubMed: 16049017]
4. Phan J, Reue K. Cell Metab. 2005; 1:73. [PubMed: 16054046]
5. Reue K. Curr Opin Lipidol. 2009; 20:165. [PubMed: 19369868]
6. Reue K, Brindley DN. J Lipid Res. 2008; 49:2493. [PubMed: 18791037]
7. Reue K, Dwyer JR. J Lipid Res. 2009; 50(Suppl):S109. [PubMed: 18941140]
8. Zeharia A, Shaag A, Houtkooper RH, Hindi T, de Lonlay P, Erez G, Hubert L, Saada A, de Keyzer Y, Eshel G, Vaz FM, Pines O, Elpeleg O. Am J Hum Genet. 2008; 83:489. [PubMed: 18817903]
9. Sirvent P, Mercier J, Lacampagne A. Curr Opin Pharmacol. 2008; 8:333. [PubMed: 18243052]
10. Allen KN, Dunaway-Mariano D. Trends Biochem Sci. 2004; 29:495. [PubMed: 15337123]
11. Allen KN, Dunaway-Mariano D. Curr Opin Struct Biol. 2009; 19:658. [PubMed: 19889535]
12. Santos-Rosa H, Leung J, Grimsey N, Peak-Chew S, Siniossoglou S. Embo J. 2005; 24:1931. [PubMed: 15889145]
13. Han GS, Siniossoglou S, Carman GM. J Biol Chem. 2007; 282(282):37026. [PubMed: 17971454]
14. Kim Y, Gentry MS, Harris TE, Wiley SE, Lawrence JC Jr, Dixon JE. Proc Natl Acad Sci U S A. 2007; 104:6596. [PubMed: 17420445]
15. Harris TE, Huffman TA, Chi A, Shabanowitz J, Hunt DF, Kumar A, Lawrence JC Jr. J Biol Chem. 2007; 282:277. [PubMed: 17105729]
16. Siniossoglou S, Santos-Rosa H, Rappsilber J, Mann M, Hurt E. Embo J. 1998; 17:6449. [PubMed: 9822591]
17. Kamenski T, Heilmeier S, Meinhart A, Cramer P. Mol Cell. 2004; 15:399. [PubMed: 15304220]
18. Yeo M, Lin PS, Dahmus ME, Gill GN. J Biol Chem. 2003; 278:26078. [PubMed: 12721286]
19. Peisach E, Selengut JD, Dunaway-Mariano D, Allen KN. Biochemistry. 2004; 43:12770. [PubMed: 15461449]
20. Galburt EA, Pelletier J, Wilson G, Stoddard BL. Structure. 2002; 10:1249. [PubMed: 12220496]
21. Zhang Y, Kim Y, Genoud N, Gao J, Kelly JW, Pfaff SL, Gill GN, Dixon JE, Noel JP. Mol Cell. 2006; 24:759. [PubMed: 17157258]

22. O'Hara L, Han GS, Peak-Chew S, Grimsey N, Carman GM, Siniossoglou S. J Biol Chem. 2006; 281:34537. [PubMed: 16968695]

23. Peterfy M, Harris TE, Fujita N, Reue K. J Biol Chem. 2010; 285:3857. [PubMed: 19955570]

24. Karanasios E, Han G-S, Xu Z, Carman GM, Siniossoglou S. Proceedings of the National Academy of Sciences. 2010; 107:17539.

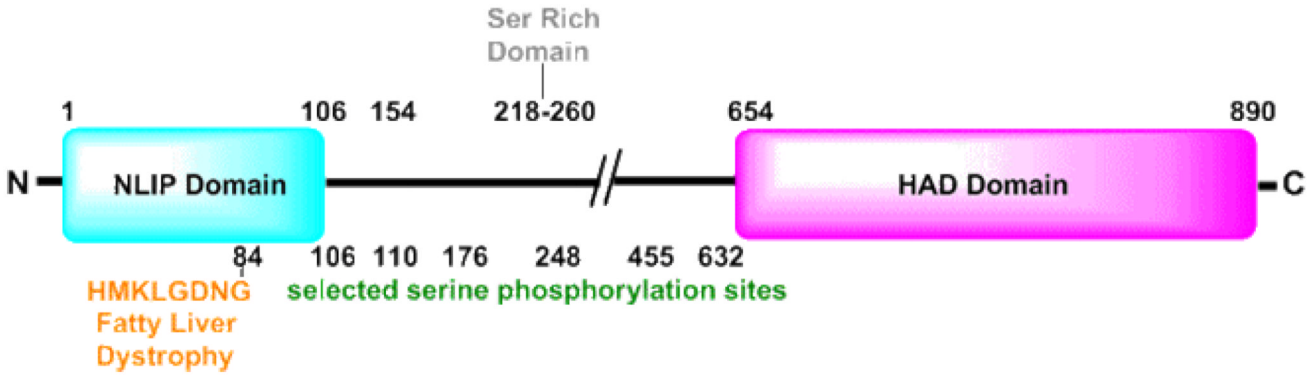

Figure 1.
Schematic diagram of human lipin1 with domains delimited. Sites of serine phosphorylation selected for peptide screening are marked.

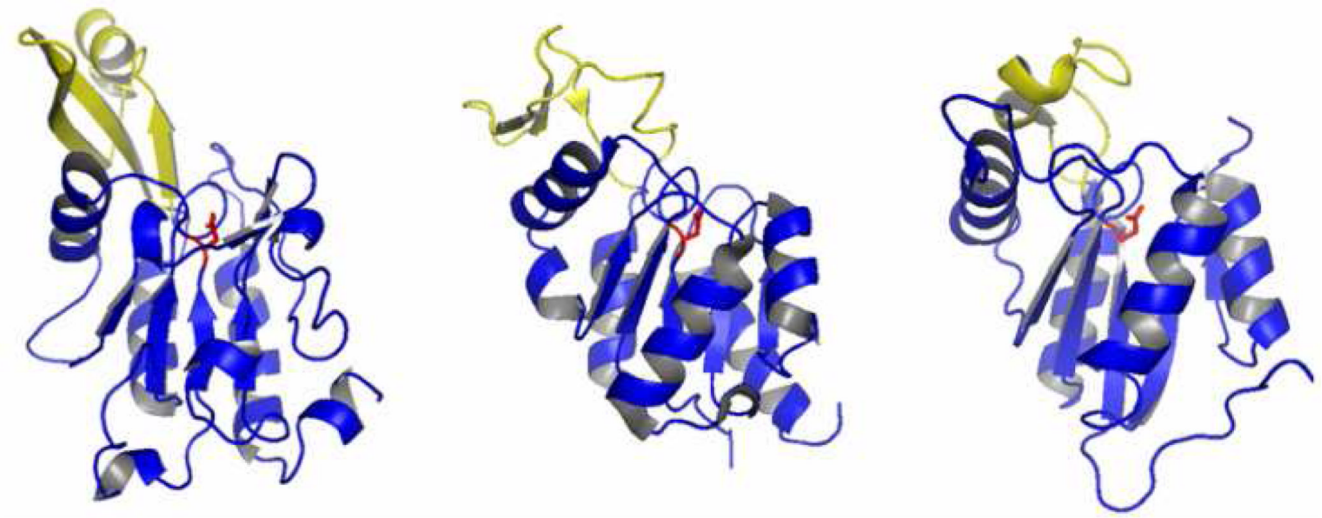

Figure 2.
Ribbon diagrams of the homology model of dullard (left), and X-ray crystal structures of Mg(II) dependent phosphatase 1 (center) and the phosphatase domain of polynucleotide kinase/phosphatase (right). The conserved Rossmann fold of the HADSF is in blue and inserted segments in yellow with the catalytic nucleophile in red to mark the active site.

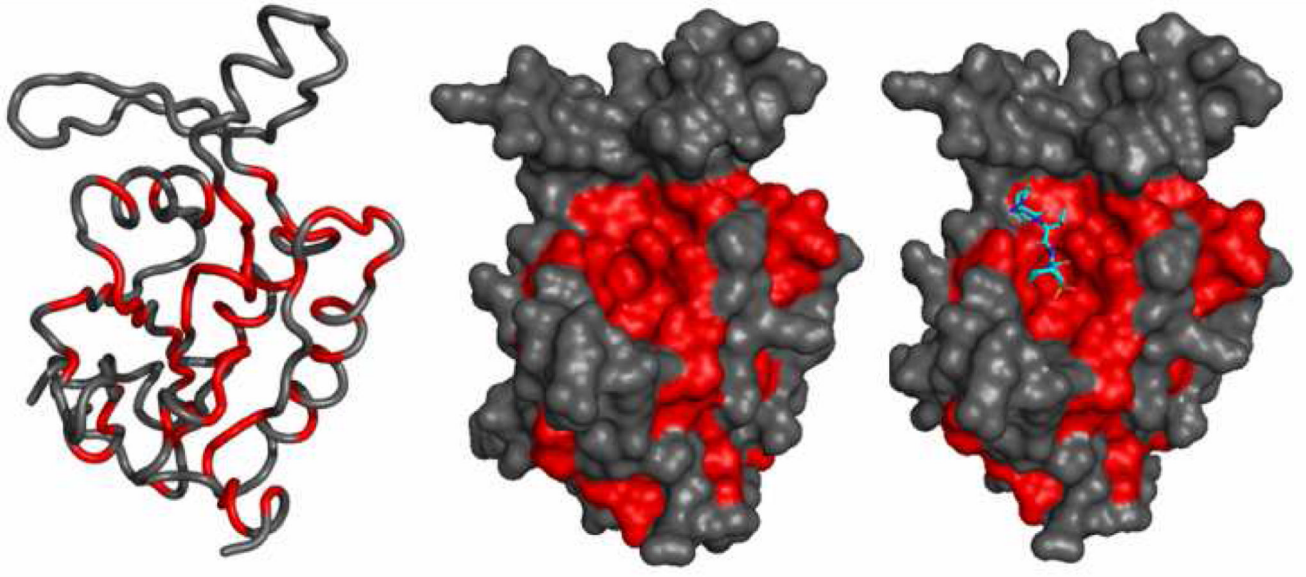

Figure 3.
Dullard model (red, stringently conserved) shown as coil (left), and spacefill (center, right) with peptide (cyan sticks) from Scp1 overlayed (right) by superimposing the Scp1 9-mer peptide complex structure (PDB 2GHQ) onto the dullard model and removing the Scp1 protein

Table 1

Steady State Kinetic Characterization of Dullard 46–244.

Lipin Derived Phosphopeptide	Peptide Sequence	K_m (μM)	k_{cat} (s^{-1})	k_{cat}/K_m ($M^{-1}s^{-1}$)
S106	HLAT(pS)PILS	32 ± 3 (50 ± 5)	0.92 ± 0.02 (1.38 ± 0.04)	2.9×10^4 (2.8×10^4)
S110	PIL(pS)EGASR	260 ± 50 (700 ± 100)	0.17 ± 0.01 (0.28 ± 0.02)	6.5×10^2 (4.0×10^2)
S176	DNMNT(pS)EDE	~ 15000	> 1 (>0.5)	
S248	SGSRP(pS)TP	32 ± 6 (700 ± 300)	0.024 ± 0.005 (0.01 ± 0.002)	7.5×10^2 (1.4×10^1)
S455	VEST(pS)DGLR	~ 10000	> 1.4 (>1.6)	
S632	LRLT(pS)EQLK	2300 ± 700 (~ 1000)	1.8 ± 0.3 (>0.5)	4.3×10^2

K_m, k_{cat} values were measured using the MESG-coupled phosphatase assay (EnzChek phosphate Assay Kit E-6646) at 25°C. Values in parentheses were measured using the Biomol Green phosphate reagent at 25 °C.